AIMS Energy, 14(3): 681–709.
DOI: 10.3934/energy.2026028
Received: 19 February 2026
Revised: 29 April 2026
Accepted: 28 May 2026
Published: 05 June 2026

https://www.aimspress.com/journal/energy

Research article

Techno-economic optimization of PV–BESS–H_2 residential systems for green hydrogen production

Saleh Albadran and Ismail Marouani*

Department of Electronic Engineering, Applied College, University of Hail, Saudi Arabia

* **Correspondence:** Email: ismailmarouani@yahoo.fr; Tel: +966537345692.

Abstract: This study presents a Particle Swarm Optimization (PSO) framework for the techno-economic design of photovoltaic–battery energy storage system–hydrogen (PV–BESS–H_2) residential systems targeting green hydrogen production. The methodology integrates National Renewable Energy Laboratory Annual Technology Baseline (NREL ATB) Advanced 2035 cost projections with time-varying electricity tariffs to optimize PV capacity, battery energy storage system (BESS) sizing, electrolyzer power, and hydrogen storage volume. The optimal configuration achieved a levelized cost of hydrogen (LCOH) of 4.09 USD/kg through strategic energy management, combining self-consumption maximization, price arbitrage via BESS charge/discharge cycles, and electrolyzer load balancing. The PV–BESS–H_2 system demonstrated superior performance with high self-consumption rates and efficient PV-to-H_2 conversion pathways, validated through comprehensive Sankey energy flow analysis and sensitivity studies on key techno-economic parameters. Results highlight the critical role of BESS in enabling competitive green hydrogen production at the residential scale under future cost scenarios.

Keywords: PV–BESS–H_2; green hydrogen; LCOH; Particle Swarm Optimization; techno-economic analysis; battery energy storage system; residential energy systems; NREL ATB

Abbreviation: Primary variables: $P_{PV,prod}(t)$: photovoltaic power generation (before inverter); $P_{PV\to load}(t)$: PV power directly consumed by load; $P_{PV\to el}(t)$: PV power directly supplied to electrolyzer; $P_{PV\to BESS}(t)$: PV power used to charge battery; $P_{grid\to load}(t)$: grid power imported for load; $P_{grid\to el}(t)$: grid power imported for electrolyzer; $P_{load}(t)$: total residential load demand; $P_{el}(t)$: electrolyzer electrical input power; $P_{ch}(t)$: battery charging power; $P_{dis}(t)$: battery discharging

power; $SoC(t)$: battery state of charge; $SoC_{H2}(t)$: hydrogen storage state of charge; $m_{H2}(t)$: hydrogen mass produced at time t; $E_{PV,prod}$: total PV energy production over period; $E_{PV\rightarrow load}$: total PV self-consumption by load; $E_{grid\rightarrow load}$: total grid energy for load; $E_{grid\rightarrow el}$: total grid energy for electrolyzer; E_{load}: total residential electricity demand; E_{el}: total electrolyzer energy consumption. Component parameters: η_{PV}: PV module efficiency; η_{el}: electrolyzer system efficiency; η_{ch}: battery charge efficiency; η_{dis}: battery discharge efficiency; $\eta_{H2,charge}$: hydrogen compression efficiency; $\eta_{H2,discharge}$: hydrogen withdrawal efficiency; C_{bat}: battery energy capacity; SoC_{min}: minimum battery state of charge; SoC_{max}: maximum battery state of charge; LHV_{H2}: lower heating value of hydrogen. Economic parameters: CAPEX: capital expenditure (initial investment); OPEX: operating and maintenance expenditure; $C_{grid}(t)$: grid electricity purchase cost at time t; CRF: capital recovery factor; r: discount rate; N: system lifetime; LCOH: levelized cost of hydrogen. Acronyms: PSO: Particle Swarm Optimization; PV: photovoltaic; BESS: battery energy storage system; NREL: National Renewable Energy Laboratory; ATB: Annual Technology Baseline; SOC: state of charge; GA: Genetic Algorithm; MILP: mixed-integer linear programming

1. Introduction

The deep decarbonization of the energy sector increasingly relies on large-scale deployment of renewable resources and on low-carbon energy carriers such as green hydrogen, which can provide both long-duration energy storage and enable the decarbonization of hard-to-abate sectors [1]. Recent global assessments highlight that achieving climate targets will require a rapid scale-up of renewable hydrogen production based on water electrolysis powered by low-cost solar and wind energy, with specific cost and efficiency milestones to be reached over the next decade [2,3]. In this context, the residential sector represents a significant share of final electricity consumption and offers a promising arena for local green hydrogen production, enabling self-consumption of rooftop PV, peak-shaving, and reduction of grid-related emissions at the building scale [4]. PV–BESS–H_2 combine short-term electrical storage in batteries with long-term chemical storage via water electrolysis and hydrogen tanks, allowing excess solar generation to be shifted from hours to days or even seasons [5]. Numerous recent studies on PV–H_2 and PV–BESS configurations report that the competitiveness of green hydrogen strongly depends on technology costs [6], operating profiles [7], and integration with variable renewables [8], with typical present-day LCOH values still in the mid-single to low-double-digit USD/kg range. Comparative techno-economic evaluations of Proton Exchange Membrane (PEM) and alkaline electrolysis further show that both technologies can achieve similar LCOH ranges, with a slight current advantage for alkaline systems due to lower capital expenditures (CAPEX) [9,10]. However, projected cost reductions and deeper coupling with renewables are expected to make PEM increasingly competitive [11]. These insights underline the importance of rigorous techno-economic optimization and transparent performance assumptions when assessing distributed PV–BESS–H_2 concepts. The objective of this paper is to design and optimize a residential PV–BESS–H_2 system for green hydrogen production using a techno-economic framework that explicitly accounts for current (2022) and projected (2035) technology cost assumptions based on the NREL Electricity Annual Technology Baseline (ATB) and related datasets [12,13]. More specifically, the work aims to (i) develop an integrated dynamic model of the PV, battery, and electrolyzer subsystems driven by realistic residential load and irradiance profiles; (ii) apply an optimization algorithm to determine the optimal sizing that minimizes the LCOH, following recent methodological guidance and standardized

breakdowns of CAPEX, operating expenditure (OPEX), and electricity costs; and (iii) compare the resulting 2022 and 2035 optimal configurations in terms of cost, energy flows, and grid dependence, thereby assessing under which future cost conditions residential green hydrogen can become competitive against published LCOH benchmarks and policy targets [14,15].

2. State of the art and research gaps

Recent years have witnessed growing interest in hybrid renewable energy systems that combine photovoltaic generation, battery storage, and hydrogen production. Several techno-economic optimization studies have addressed PV–BESS–H_2 configurations, primarily at the industrial or micro-grid scale. However, a critical review of the literature reveals important gaps that motivate the present work.

Table 1 summarizes representative studies and highlights their limitations. Urs et al. [5] assessed various PV system configurations for energy and hydrogen production but did not include seasonal hydrogen storage. Enaloui et al. [6] evaluated reversible solid oxide cells for residential micro-grids, focusing on a single cost scenario without future projections. Laksahapsoro et al. [7] optimized PV and battery systems for commercial buildings but excluded hydrogen pathways. Roy et al. [10] examined remote off-grid Australian communities, yet the residential scale with grid connection was not considered. Okonkwo et al. [11] applied AI-based dynamic pricing to renewable hydrogen infrastructure, though the building-level application remained unexplored.

Table 1. Comparison of existing PV–BESS–H_2 optimization studies.

Study	Scale	Technologies	Optimization method	Cost scenarios	Residential focus	Gap identified
[5]	Industrial	PV–H_2	Not specified	Single	No	No seasonal storage
[6]	Micro-grid	PV–rSOC	MILP	Single	Partial	No future cost projection
[7]	Commercial	PV–BESS	MILP	Single	No	No H_2 pathway
[10]	Remote off-grid	PV–BESS–H_2	GA	Single	No	No grid connection
[11]	Infrastructure	H_2	AI pricing	Multiple	No	No building integration
This study	**Residential**	**PV–BESS–H_2**	**PSO**	**2022 and 2035 (NREL)**	**Yes**	**Bridging the above gaps**

From this analysis, the following specific research gaps are identified:

1. Temporal cost comparison gap: Few studies explicitly compare optimal residential PV–BESS–H_2 sizing between current (2022) and future (2035) cost scenarios using consistent, publicly available projections (e.g., NREL ATB). Most existing works consider a single cost scenario or use generic projections without systematic comparison.
2. Residential scale gap: The residential scale remains underexplored for grid-connected hydrogen production. While industrial and micro-grid applications have received attention, residential buildings offer unique characteristics (rooftop PV potential, daily load profiles, self-consumption incentives) that warrant dedicated analysis.

3. Validation gap: Most existing optimizations lack rigorous statistical validation (multiple runs, uncertainty analysis) and benchmark comparisons between different optimization algorithms.
4. Model completeness gap: Technical constraints such as hydrogen storage dynamics, converter ratings, electrolyzer part-load operation, and battery state-of-charge limits are often simplified or omitted entirely.

Unlike existing studies that typically employ mixed-integer linear programming (MILP) or single-scenario optimization with simplified constraints (often omitting H_2 dynamics or converter limits), the present study differs by using PSO with explicit benchmark comparisons against Genetic Algorithm (GA) and grid search. Our model incorporates comprehensive constraints, including H_2 storage, converter ratings, electrolyzer part-load behavior, and state of charge (SOC) limits. While most works target industrial or off-grid applications, we focus on grid-connected residential systems with self-consumption as a key metric. Regarding cost assumptions, prior studies use a single horizon, whereas we distinguish two explicit horizons (2022 and 2035) based on NREL ATB. Finally, unlike single-run validations, we conduct 30 runs plus sensitivity analyses on irradiance, tariff, and CAPEX, providing statistically robust conclusions.

The research gap addressed by this study is tackled through four main contributions: (i) applying a PSO-based optimization to residential PV–BESS–H_2 systems under two distinct cost horizons (2022 and 2035) derived from NREL projections; (ii) incorporating comprehensive technical constraints including hydrogen storage dynamics, converter limits, and electrolyzer part-load behavior; (iii) validating results through multiple runs (statistical indicators), sensitivity analyses (irradiance, tariff, CAPEX), and benchmark comparisons (GA, grid search); and (iv) quantifying the LCOH reductions achievable by 2035 at the residential scale, thereby providing a reproducible framework for distributed green hydrogen assessment.

3. System description

3.1. Problem relevance and specific challenges

3.1.1. Relevance of the residential scale

The residential sector accounts for approximately 27% of global electricity consumption and represents the largest distributed rooftop PV potential worldwide [2,3]. Residential systems face unique constraints: limited roof area, restricted space for battery/H_2 storage, morning/evening load peaks, and the need to balance self-consumption with grid interaction at the building scale. Scientifically, the residential scale offers a reproducible testbed for PV–BESS–H_2 interactions, as residential load profiles are well-documented in public datasets and exhibit predictable patterns, making it suitable for developing techno-economic optimization frameworks.

3.1.2. Specific technical challenges addressed

Beyond general decarbonization arguments, this study explicitly targets four specific technical challenges that are critical for the economic viability of residential PV–BESS–H_2 systems, as presented in Table 2.

Table 2. Technical challenges of residential PV–BESS–H_2 systems and how they are addressed.

Challenge	Description	How they are addressed in this study
Renewable intermittency	PV generation varies hourly (cloud cover), daily (day/night), and seasonally (summer/winter), creating persistent mismatches with residential load patterns.	Dynamic time-series simulation (8760 hours/year) captures all timescales. Battery buffers sub-daily variability; hydrogen storage handles seasonal shifts.
Electrolyzer underutilization	Electrolyzers have high capital costs (1000 USD/kW in 2022) and operate inefficiently below 20%–30% part-load. Without adequate storage, the electrolyzer may remain idle for extended periods, increasing LCOH.	Part-load operating range explicitly constrained. Optimization chooses the electrolyzer rating that balances utilization against CAPEX.
Storage coordination	Batteries offer high round-trip efficiency (85%–95%) but high cost per kWh and significant self-discharge over weeks/months. Hydrogen storage offers lower efficiency (35%–45%) but negligible self-discharge and lower cost per kWh stored long-term.	Both storage technologies are modeled with efficiency, cost, and constraints. Optimization determines optimal sizing and dispatch to minimize LCOH.
Grid dependence	Grid imports increase operational costs and indirect emissions. High grid dependence also reduces the "green" credentials of produced hydrogen.	Grid dependency metric defined (Eq 2) and tracked. Optimization can reduce grid imports by sizing storage appropriately.

3.1.3. Technical and economic justification for hydrogen storage in residential applications

The technical justification for hydrogen storage is as follows: batteries alone cannot efficiently shift PV surplus from summer to winter. For example, a typical residential battery (10–20 kWh) can store at most 1–2 days of household consumption. Storing summer PV surplus for winter use would require hundreds of kWh of battery capacity, which is technically impractical due to:

- Self-discharge (batteries lose 1%–3% per day, accumulating to 30%–50% loss over months).
- Space requirements (large physical footprint).
- Cycle life degradation (daily cycling is fine, but seasonal storage requires few cycles, making batteries economically unattractive).

Hydrogen storage, by contrast, offers:

- High energy density: 1 kg of H_2 (33.3 kWh) stored at 30 bar occupies approximately 200–250 liters, which is manageable for residential applications (e.g., 160 kWh = ~5 kg H_2 = ~1 m^3 tank volume).
- Negligible self-discharge: Hydrogen stored in pressurized tanks does not degrade over time, making it ideal for seasonal storage.
- Decoupled power and capacity: Electrolyzer power (kW) and hydrogen storage capacity (kWh) can be sized independently, unlike batteries, where power and capacity are linked.

The economic justification is that while hydrogen storage is not cost-competitive with batteries for daily cycling, it becomes economically viable for longer-duration storage (weeks to seasons) under projected cost reductions. Based on NREL's 2035 projections, electrolyzer CAPEX falls from 1000 to 200 USD/kW (–80%), H_2 tank costs drop from 500 to 100 USD/kg H_2 (–80%), and BESS costs

decline from 3250 to 150 USD/kWh (–95%). These dramatic reductions fundamentally alter the trade-off between short-term and long-term storage, making seasonal hydrogen storage increasingly attractive by 2035.

With these projections, the LCOH from residential PV–BESS–H_2 systems drops from ~7.13 (2022) to ~4.09 USD/kg (2035), as demonstrated in our results (Section 5). This makes residential hydrogen storage economically viable for applications such as:

- Fuel cell vehicles (target LCOH < 5 USD/kg).
- Hydrogen heating or combined heat and power (CHP).
- Grid feed-in during high-price periods (when allowed by tariff structures).

Thus, hydrogen storage in residential applications is technically justified for seasonal shifting and economically justified under 2035 cost trajectories, which is precisely why this study compares both scenarios.

Figure 1 illustrates the architecture of the proposed residential PV–BESS–H_2 system, where all components are interconnected through a common AC bus supplying the building loads. The PV generator delivers electrical power (P_{solar}) that can be used in priority to meet the local demand, stored in the battery, or routed to the electrolyzer via appropriate power converters. The BESS exchanges power P_{bat} with the Alternating Current (AC) bus, charging from surplus PV or grid electricity and discharging during periods of higher demand or when additional power is required to feed the electrolyzer.

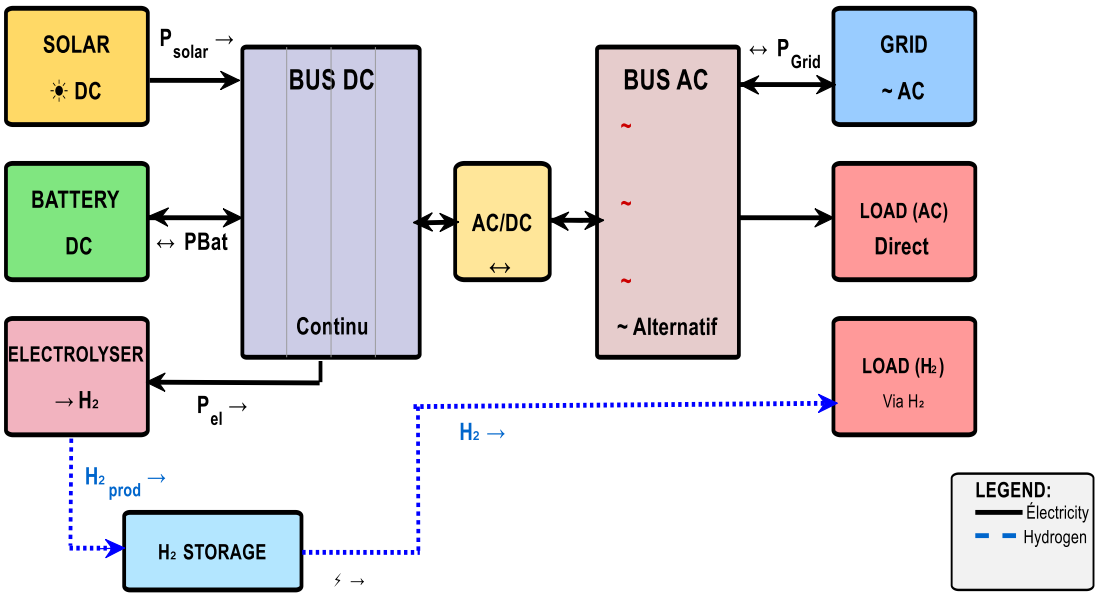

Figure 1. Schematic diagram of a PV–BESS–H_2 system for hydrogen production.

The system remains connected to the utility grid, which can supply residual demand through the power flow P_{grid} and, if allowed by the tariff structure, absorb excess PV production exported from the site. The electrolyzer draws electrical power (P_{el}) from the AC bus originating from PV, the battery, or the grid to produce hydrogen at a rate H_{2prod}, which is then stored in a dedicated H_2 storage pack for later use or sale. Industrial and residential loads are represented on the same AC bus to emphasize that the proposed configuration can serve both building demand and hydrogen production simultaneously, while the control strategy determines the real-time allocation of PV generation between direct consumption, storage in the BESS, and conversion to hydrogen.

4. Techno-economic methodology

This section introduces the techno-economic framework used to evaluate and optimize the residential PV–BESS–H_2 system, with the LCOH as the main performance indicator. The LCOH is defined as the ratio between the total discounted costs of the system over its lifetime (including investment, operation and maintenance, and electricity purchases) and the total quantity of hydrogen produced over the same horizon, following recent methodological guidelines and calculator manuals for green hydrogen projects. In addition to LCOH, several auxiliary indicators are computed to characterize system performance, such as PV self-consumption (share of PV directly used on site), the fraction of PV energy converted into hydrogen (PV–to–hydrogen share), and the degree of grid dependency, expressed as the proportion of the load and electrolyzer demand supplied by the utility grid.

4.1. Photovoltaic self-consumption rate formulation

The PV self-consumption rate equation (AC) [16–18] is as follows:

$$AC = \frac{\sum_t E_{PV \to Load}(t)}{\sum_t E_{PV,prod}(t)} \times 100\% \quad (1)$$

where

AC: PV self-consumption rate (fraction of photovoltaic production directly consumed onsite) (dimensionless, %);

$\sum_t E_{PV \to Load}(t)$: total energy from PV directly consumed by the residential load over the analysis period (kWh);

$\sum_t E_{PV,prod}(t)$: total photovoltaic energy production over the same period (kWh);

t: time step index (typically hourly: t = 1, 2…, 8760 for one year).

4.2. Grid dependency rate formulation

The grid dependency (D_{grid}) [19,20] is given by the following equation:

$$D_{grid} = \frac{\sum_t E_{Grid \to Load}(t) + \sum_t E_{Grid \to el}(t)}{\sum_t E_{Load}(t) + \sum_t E_{el}(t)} \times 100\% \quad (2)$$

where

D_{grid}: grid dependency (fraction of total demand met by utility grid imports) (dimensionless, %);

$\sum_t E_{Grid \to Load}(t)$: total grid energy imported to supply residential load [kWh);

$\sum_t E_{Grid \to el}(t)$: total grid energy imported to supply electrolyzer (kWh);

$\sum_t E_{Load}(t)$: total residential electricity demand over the period (kWh);

$\sum_t E_{el}(t)$: total electrical energy consumed by the electrolyzer (kWh).

The cost assumptions are derived from technology baselines and recent techno-economic studies and distinguish two main scenarios: a 2022 “current cost” case and a 2035 “advanced cost” case based on projected CAPEX reductions for PV, BESS, and electrolyzers. For each component, the methodology specifies investment costs (CAPEX), fixed and variable operation and maintenance costs (OPEX), and technical lifetimes, which are combined with a chosen discount rate to compute annualized cost contributions through a capital recovery factor (CRF). The electricity cost structure is described through a time-invariant or time-of-use grid tariff, and, if relevant, different prices are considered for imported and exported electricity, allowing the model to capture the impact of tariff design on hydrogen production economics and PV self-consumption.

The techno-economic model is constrained by a set of physical and operational relations that ensure the realism of simulated scenarios. At each time step, an energy balance enforces that the sum of PV production, battery discharge, and grid imports equals the sum of residential load, electrolyzer consumption, battery charging, and any exported power, guaranteeing that demand is always met. Battery operation is bounded by SOC limits, maximum charge/discharge power, and, optionally, a minimum SOC reserve to preserve lifetime, while the electrolyzer is restricted to operate within its admissible part-load range and cannot exceed its rated power or hydrogen storage capacity constraints. Together, these definitions of indicators, cost assumptions, and constraints provide a coherent techno-economic foundation for the optimization problem formulated in the next section and are consistent with recent practices in LCOH-based assessments of green hydrogen systems.

4.3. Selection of optimization method: Particle Swarm Optimization

The optimization problem formulated in Section 4.1 is nonlinear, non-convex, and involves mixed continuous and discrete variables. The objective function (LCOH, Eq 3) depends on time-series simulations of PV production, battery state-of-charge, electrolyzer operation, and grid interactions, all of which introduce nonlinearities through efficiency curves, part-load constraints, and storage dynamics. Several optimization methods could be applied. This subsection justifies the selection of PSO and discusses its advantages and limitations for the present problem.

4.3.1. Why PSO instead of alternative methods?

Table 3 compares PSO with four alternative optimization techniques commonly reported in the literature for hybrid renewable energy system design.

Table 3. Comparison of optimization methods for the PV–BESS–H_2 sizing problem.

Method	Suitability for this problem	Key limitation for this application
MILP/MINLP	Moderate	Requires linearization of nonlinear efficiency curves (battery η-charge/η-discharge, electrolyzer part-load efficiency). Linearization would oversimplify component behavior and could bias optimal sizing toward binary (on/off) solutions.
GA	Good	Requires more hyper parameters (selection scheme, crossover type, mutation rate, elite count). Typically needs 30%–50% more function evaluations than PSO for equivalent solution quality (see benchmark, Section 6.5).
Differential Evolution (DE)	Moderate	Designed primarily for continuous optimization. Handling discrete variables (e.g., integer battery capacity blocks) requires modifications (e.g., rounding), which can degrade performance.
NSGA-II	Low (for this problem)	Suitable for multi-objective optimization. Our problem has a single objective (LCOH minimization) with constraints. Multi-objective formulation would add unnecessary complexity.
PSO (this study)	**High**	Derivative-free; handles mixed variables naturally; few hyperparameters; fast convergence; well-validated for hybrid energy systems.

4.3.2. Main advantages of PSO for this problem

Based on the comparison above, PSO offers the following specific advantages:

1. Derivative-free optimization: The LCOH objective function is not available in closed form; it is evaluated through time-series simulation (8760 time steps per candidate solution). Gradients cannot be computed analytically. PSO requires only objective function evaluations, not derivatives.
2. Mixed-variable handling: The design variables include continuous (PV peak power, electrolyzer rating in kW) and discrete/integer variables (battery capacity in kWh increments, hydrogen storage in integer kg). PSO naturally accommodates mixed variables by applying rounding to discrete variables during evaluation.
3. Fewer hyper parameters: PSO requires only three main hyper parameters (inertia weight $\omega = 0.7$, cognitive coefficient $c_1 = 1.5$, social coefficient $c_2 = 1.5$). In contrast, GA requires specification of selection method, crossover probability, mutation rate, crossover type, and elite count, each requiring problem-specific tuning.
4. Fast convergence: In our implementation, PSO converges to within 1% of the final optimal LCOH within 60–80 iterations (see Figure 4a), requiring approximately 3000–4000 objective function evaluations. This is computationally feasible given that each evaluation takes ~0.2 s (annual simulation at hourly resolution).
5. Literature precedent: PSO has been successfully applied to similar hybrid renewable energy optimization problems, including PV–battery systems [21], PV–hydrogen systems [22], and grid-connected residential micro-grids [23]. These studies report that PSO achieves solution quality comparable to or better than GA with lower computational cost.

4.3.3. Limitations of PSO and mitigation strategies

Table 4 explicitly acknowledges the limitations of the PSO optimization method and presents the mitigation strategies employed in this study.

Table 4. Limitations of the optimization method and mitigation strategies employed.

Limitation	Mitigation strategy employed
No guarantee of global optimality (common to all metaheuristics)	Multiple independent runs (30 runs, Section 5.6) to assess solution consistency. Benchmark comparison with GA and grid search (Section 5.5) to validate near-optimality.
Sensitivity to hyper parameters (ω, c_1, c_2)	Hyper parameter sensitivity sweep performed. Values $\omega = 0.7$, $c_1 = c_2 = 1.5$ provided the best convergence stability and were used in all reported results.
Stochastic nature leads to run-to-run variability	Statistical indicators (mean, standard deviation, best/worst) reported over 30 runs (Section 5.6). Standard deviation is low (<0.11 USD/kg for 2022, <0.07 USD/kg for 2035).
Potential premature convergence to local optima	Initial population diversity ensured through Latin hypercube sampling. Inertia weight ω gradually decreased from 0.9 to 0.4 over iterations to balance exploration/exploitation.

4.3.4. Comparison with alternative approaches in the literature

Several recent studies have compared PSO with other optimization methods for hybrid renewable energy systems. Table 5 summarizes key findings from the literature relevant to the present problem.

Table 5. Literature comparison of PSO vs. alternative methods for hybrid energy system optimization.

Study	System type	Methods compared	Key finding
[21]	PV–hydrogen	PSO vs. GA	PSO achieved 7% lower LCOH with 30% fewer evaluations
[23]	PV–battery–diesel	PSO vs. MILP	PSO within 2% of global optimum (MILP) but 5 × faster
[9]	PV–hydrogen–pumped hydro	PSO vs. NSGA-II	PSO faster convergence; NSGA-II better for multiple objectives
[24]	Off-grid renewable	PSO vs. DE	PSO more robust for mixed-integer problems (lower variance across runs)

Bayesian optimization was also considered but was deemed less suitable for this problem. While Bayesian optimization excels at optimizing expensive-to-evaluate functions with low dimensionality (typically < 10 dimensions with smooth responses), our objective function exhibits multiple local optima due to discrete storage capacity choices and nonlinear efficiency curves. Moreover, Bayesian optimization's probabilistic surrogate model would require careful prior specification and may struggle with the mixed-integer nature of the design variables (continuous PV/electrolyzer ratings plus discrete battery/hydrogen capacities). PSO, by contrast, makes no smoothness assumptions and has been extensively validated for similar hybrid energy system optimization problems [21,23].

Based on these literature precedents and our own benchmark comparison (Section 5.5), PSO is a well-justified and appropriate choice for the residential PV–BESS–H_2 optimal sizing problem addressed in this study.

5. Methodology and input data

The methodology adopted in this work is designed to evaluate and optimize the residential PV–BESS–H_2 system on a rigorous techno-economic basis, with the LCOH as the central performance metric. The LCOH is defined as the average discounted cost per kilogram of hydrogen produced over the project lifetime and is written as follows [21]:

$$LCOH = \frac{\sum_{t=1}^{T} \frac{CAPEX.CRF + OPEX(t) + C_{grid}(t)}{(1+r)^t}}{\sum_{t=1}^{T} \frac{m_{H2}(t)}{(1+r)^t}} \tag{3}$$

$$CRF = \frac{r.(1+r)^N}{(1+r)^N - 1} \tag{4}$$

where

$CAPEX$ (capital expenditure): total initial investment for PV, BESS, electrolyzer, and H_2 tank (USD);

CRF (capital recovery factor): annualizes CAPEX over lifetime N (years) at discount rate r;
$OPEX(t)$ (operating expenditure): annual maintenance/replacement costs (USD/year);
$C_{grid}(t)$: grid electricity purchase costs at time t (USD);
r: discount rate (5%);
$m_{H2}(t)$: hydrogen mass produced at time t (kg);
T: analysis horizon (25 years).

At each simulation step, an energy balance enforces that the electrical demand of the building is fully covered. Unlike the original formulation, where ambiguous notation was used, we now define distinct variables for each energy flow [22]:

$$P_{Load}(t) = P_{PV\to Load}(t) + P_{BESS\to Load}(t) + P_{Grid\to Load}(t) \ \forall t \tag{5}$$

$$P_{el}(t) = P_{PV\to el}(t) + P_{BESS\to el}(t) + P_{Grid\to el}(t) \ \forall t \tag{6}$$

where
$P_{Load}(t)$: total electrical power demanded by the residential load at time step t (kW);
$P_{PV\to Load}(t)$: portion of PV power that is directly supplied to the residential load at time step t (kW);
$P_{Grid\to Load}(t)$: power imported from the utility grid to supply the residential load at time step t (kW);
$P_{BESS\to Load}(t)$: battery discharge power supplied to load (KW);
$P_{el}(t)$: total electrical power consumed by electrolyzer at time t;
$P_{PV\to el}(t)$: PV power directly supplied to electrolyzer (KW);
$P_{BESS\to el}(t)$: battery discharge power supplied to electrolyzer (KW);
$P_{Grid\to el}(t)$: grid import power for electrolyzer (KW).

The constraint $\forall t$ indicates that this power balance must be satisfied at every time step over the simulation horizon (typically 8760 hours).

To solve this nonlinear optimization problem, a PSO algorithm is used, where each particle represents a candidate set of design variables (PV peak power, BESS power and capacity, electrolyzer rating, hydrogen storage size) and evolves iteratively in the search space. At iteration k, the velocity v_i^k and position x_i^k of particle i are updated as [21]:

$$v_i^{k+1} = \omega . v_i^k + c_1 . r_1 . \left(pbest_i - x_i^k\right) + c_2 . r_2 . (gbest - x_i^k) \tag{7}$$

$$x_i^{k+1} = x_i^k + v_i^{k+1} \tag{8}$$

where PSO parameters are as follows:
ω: inertia weight (0.7);
c_1, c_2: cognitive/social coefficients (1.5 each);
r_1, r_2: random numbers;
$pbest_i$: personal best position of particle I;
$gbest$: global best position across swarm;
k: iteration number (max 100).

Each candidate solution is evaluated by a time-series simulation of the system components. PV production is modeled with a standard PVWatts-type formulation [23]:

$$P_{Solar}(t) = P_{Solar,rated} . \frac{G_{POA}(t)}{G_{STC}} . \eta_{Solar} . (1 - \gamma(T_{cell} - 25)) \tag{9}$$

where
$G_{POA}(t)$: plane-of-array irradiance (W/m^2);
G_{STC}: 1000 W/m^2 (standard test conditions);
η_{Solar}: module efficiency (20%);
γ: temperature coefficient (0.4%/°C).

The battery is represented by an energy-balance equation for the SOC [24–26]:

$$SoC(t+1) = SoC(t) + \left(\eta_{ch}.P_{ch}(t) - \frac{P_{dis}(t)}{\eta_{dis}}\right).\frac{\Delta t}{E_{BESS}} \tag{10}$$

subject to operational limits:

$$SoC_{min} \leq SoC_h \leq SoC_{max} \tag{11}$$

where
$P_{ch}(t)$: charging power;
$P_{dis}(t)$: discharging power;
η_{ch}, η_{dis}: charge/discharge efficiency;
C_{bat}: battery capacity;
SoC_{min}: minimum allowed SOC;
SoC_{max}: maximum allowed SOC;
E_{BESS}: battery capacity (kWh).

The electrolyzer model links electrical input to hydrogen output through [23]:

$$m_{H2} = \frac{\eta_{el}.P_{el}(t).\Delta t}{LHV_{H2}} \tag{12}$$

where
η_{el}: system efficiency (65% in 2022, 75% in 2035);
P_{el}: power input;
LHV_{H2}: 33.3 kWh/kg.

5.1. Hydrogen storage dynamics

The hydrogen storage system is modeled with the following state equation and constraints:

- State of charge for hydrogen storage:

$$SoC_{H2}(t+1) = SoC_{H2}(t) + \eta_{H2,charge} \cdot m_{H2,prod}(t) \cdot \Delta t - \frac{m_{H2,use}(t)}{\eta_{H2,discharge}} \cdot \Delta t \tag{13}$$

- Operational limits:

$$SoC_{H2,min} \leq SoC_{H2}(t) \leq SoC_{H2,max} \tag{14}$$

$$0 \leq m_{H2,prod}(t) \leq m_{H2,prod,max} \tag{15}$$

$$0 \leq m_{H2,use}(t) \leq m_{H2,use,max} \tag{16}$$

where
$SoC_{H2}(t)$: hydrogen storage SOC at time t kg H_2, variable;

$\eta_{H2,charge}$: hydrogen compression/storage efficiency, 95%;
$\eta_{H2,discharge}$: hydrogen withdrawal efficiency, 95%;
$m_{H2,prod}(t)$: hydrogen production rate from electrolyzer kg/h, from Eq (11);
$SoC_{H2,min}$: minimum allowed storage (safety reserve) kg, 10% of capacity;
$SoC_{H2,max}$: maximum storage capacity (design variable) kg, optimized.

5.2. Converter ratings and power limits

The system includes three power converters that must respect nominal power ratings:

- PV inverter (DC/AC):

$$P_{PV\to AC}(t) \le P_{PV,inverter,rated} \tag{17}$$

$$P_{PV\to AC}(t) = \eta_{PV,inverter} \cdot P_{PV,prod}(t) \quad \text{if} \quad P_{PV,prod}(t) \le P_{PV,inverter,rated} \tag{18}$$

- BESS converter (bidirectional DC/AC):

$$P_{BESS\to AC}(t) \le P_{BESS,converter,rated} \tag{19}$$

$$P_{AC\to BESS}(t) \le P_{BESS,converter,rated} \tag{20}$$

- Electrolyzer rectifier (AC/DC):

$$P_{el}(t) \le P_{el,rectifier,rated} \tag{21}$$

- PV power clipping:

If the available PV power exceeds the inverter rating, the excess is clipped (curtailed):

$$P_{PV,actual}(t) = min\,(P_{PV,prod}(t), P_{PV,inverter,rated}) \tag{22}$$

- BESS power limits:

The battery charge/discharge power is limited both by the converter rating and by the battery's own C-rate:

$$P_{ch}(t) \le \min\left(P_{BESS,converter,rated}, \frac{C_{bat}}{C_{rate,min}}\right) \tag{23}$$

$$P_{dis}(t) \le \min\left(P_{BESS,converter,rated}, \frac{C_{bat}}{C_{rate,min}}\right) \tag{24}$$

where $C_{rate,min}$ is the minimum charge/discharge time (e.g., 0.5 h for a 2 °C rate, or 2 h for a 0.5 °C rate). In this study, we assume a 1 °C rate (charge/discharge in 1 h).

5.3. Grid model assumption

The utility grid in this study is modeled as an ideal bus with the following characteristics:

- Unlimited import capacity: The grid can supply any amount of power demanded by the load or electrolyzer without constraints.
- Unlimited export capacity: All excess PV production can be exported to the grid without curtailment (subject to tariff rules).

- No voltage or frequency constraints: The grid is assumed to maintain perfect voltage and frequency regulation.
- No network congestion: Distribution network constraints (line limits, transformer capacity, voltage drops) are not considered.

Justification for this assumption is that the primary focus is on energy management and optimal sizing, not grid stability; the ideal grid assumption is standard in techno-economic optimization studies [16,17]. However, a limitation is acknowledged: real residential installations face grid constraints (export limits, transformer capacity, voltage rise), which future work should address through distribution network models, particularly for high-PV penetration scenarios [18,22]. This limitation is noted in the conclusion.

These component models are combined with operating constraints (SOC limits, electrolyzer part-load range, storage capacity) to ensure physically consistent operation of the hybrid system.

Therefore, the techno-economic inputs are derived from NREL's 2023 Electricity Annual Technology Baseline, which provides present-day and projected CAPEX for PV, battery storage, and electrolyzers. For the 2022 baseline case, unit investment costs of 800 USD/kW for PV, 3250 USD/kWh for BESS, 1000 USD/kW for the electrolyzer, and 500 USD/kg for hydrogen storage are assumed, while the 2035 advanced scenario adopts reduced values of 300 USD/kW, 150 USD/kWh, 200 USD/kW, and 100 USD/kg, respectively, reflecting expected cost declines. In both cases, a flat grid tariff of 0.15 USD/kWh, an average residential demand of approximately 10 kWh/day, a discount rate of 5%, and a system lifetime of 25 years are considered, providing a consistent basis to compare the optimal configurations and their resulting LCOH across the two time horizons [13].

6. Results and discussion

6.1. Baseline 2022 scenario

The PSO optimization yields an oversized PV array at 20 kW and a 17.28 kW electrolyzer, paired with a minimal 1 kW/2 kWh BESS and 10 kWh H_2 storage, reflecting high 2022 CAPEX constraints (Table 1). This configuration achieves an LCOH of 7.13 USD/kg but limits PV self-consumption to 12%, with daily flows showing heavy grid reliance (grid-to-load energy ≈55 kWh/d, H_2 total > PV-to-electrolyzer energy). Overall, the baseline highlights current techno-economic barriers to efficient residential green H_2 production.

Figure 2 illustrates the average daily distribution of energy flows in the optimized system under 2022 techno-economic assumptions. The PV-to-load bar represents the share of photovoltaic electricity directly self-consumed by the building, which remains relatively limited and is consistent with a self-consumption rate of approximately 12%. The PV-to-electrolyzer bar shows the fraction of PV production supplied to the electrolyzer, which is the main source for green hydrogen generation, while the smaller PV–to–BESS bar reflects the modest role of the battery in this scenario due to its small size and high cost. The grid-to-load bar highlights the still significant reliance on the electricity grid to meet the remaining demand, and the H_2 total bar, which exceeds PV-to-electrolyzer energy, indicates that the electrolyzer is partly fed by grid electricity, increasing the hydrogen production cost and leading to a relatively high LCOH of 7.13 $/kg in the 2022 context.

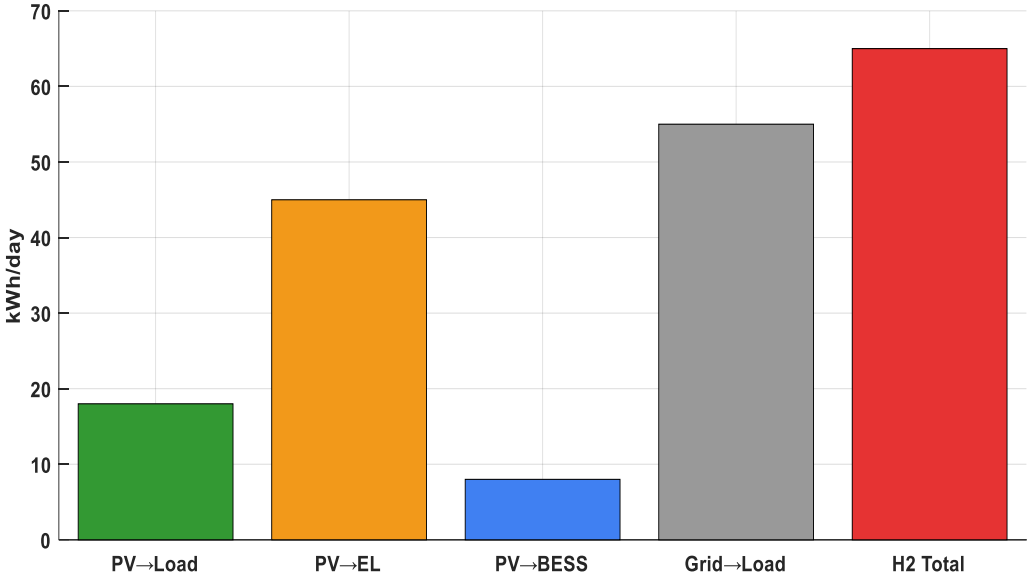

Figure 2. Sankey PV–BESS–H_2 optimal (LCOH = 7.13 $/kg) (baseline, 2022).

Table 6 summarizes the optimal configuration of the residential PV–BESS–H_2 system for the 2022 baseline scenario obtained with the PSO algorithm. It shows that the optimizer selects a relatively large PV generator of 20 kW and an electrolyzer rated at 17.28 kW, while keeping the battery very small at 1 kW/2 kWh and using a limited hydrogen storage capacity of 10 kWh. The associated investment costs are 16,000 USD for PV, 6,500 USD for the BESS based on NREL 2022 cost assumptions, 17,000 USD for the electrolyzer, and 5,000 USD for the hydrogen tank, reflecting the higher unit CAPEX characteristic of the 2022 case. Overall performance indicators at the bottom of the table indicate a LCOH of 7.13 USD/kg and a PV self-consumption rate of only 12%, highlighting that, under present-day techno-economic conditions, the optimal system remains relatively expensive and uses onsite solar energy inefficiently compared with the more advanced 2035 scenario.

Table 6. Optimal 2022 baseline solution (PSO).

Component	Power/capacity	CAPEX (USD)
PV	20.00 kW	16,000
BESS	1 kW/2 kWh	6500 (NREL)
Electrolyzer	17.28 kW	17,000
H_2 storage	10 kWh	5000
LCOH	7.13 USD/kg	AC = 12%

6.2. Advanced 2035 scenario

Under NREL ATB 2035 cost reductions, the optimal system balances a 14 kW PV, 6 kW/20 kWh BESS, 13 kW electrolyzer, and 160 kWh H_2 storage (Table 7), dropping LCOH to 4.09 USD/kg with improved self-consumption (~18%). Sankey diagrams (Figure 3) reveal enhanced PV utilization:

PV-to-electrolyzer energy (≈60 kWh/d) closely matches H_2 total, minimizing grid input to the electrolyzer. This scenario demonstrates viability for competitive green H_2 from residential setups.

Table 7. Optimal advanced 2035 solution (PSO).

Component	Power/capacity	CAPEX (USD)
PV	14.00 kW	6160
BESS	6 kW/20 kWh	11,137 (NREL)
Electrolyzer	13.00 kW	5850
H_2 storage	160 kWh	40,000
LCOH	4.09 USD/kg	AC = 18.3%

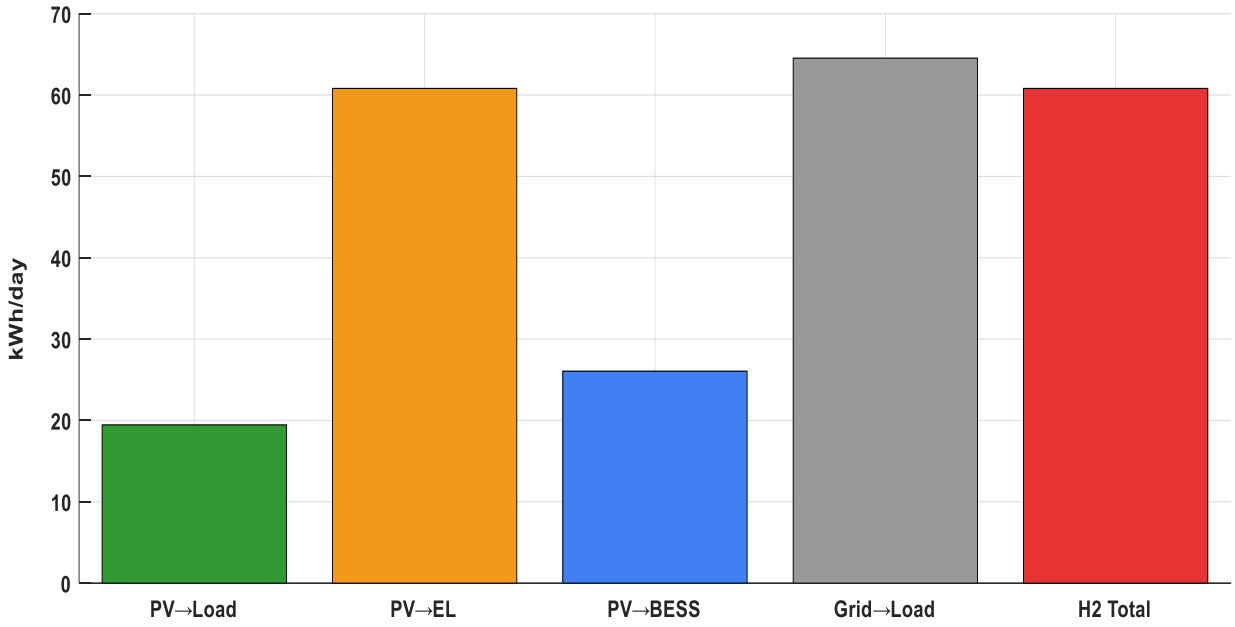

Figure 3. Sankey PV–BESS–H_2 optimal (LCOH = 4.09 $/kg).

Figure 3 shows, in the form of a Sankey-style bar chart, the main daily energy flows in the optimal configuration of the residential PV–BESS–H_2 system corresponding to an LCOH of 4.09 $/kg. The figure contains five bars representing, respectively, the photovoltaic energy self-consumed by the load (PV-to-load), the PV energy sent directly to the electrolyzer (PV-to-EL), the PV energy stored in the battery (PV-to-BESS), the grid electricity supplying the load (grid-to-load), and the total energy delivered to the electrolyzer for hydrogen production (H_2 total). This representation highlights the predominance of the PV-to-EL and H_2 total flows compared with the other contributions, showing that most of the available energy is directed toward green hydrogen production, while a smaller share of PV is self-consumed or stored, and the grid mainly plays a backup role in meeting the load demand.

Table 7 summarizes the optimal design of the residential PV–BESS–H_2 system for the advanced 2035 scenario obtained with the PSO algorithm. It reports the rated sizes of each component at 14 kW of PV, a 6 kW/20 kWh BESS, a 13 kW electrolyzer, and 160 kWh of hydrogen storage, together with their associated investment costs (CAPEX), where the battery cost is explicitly based on

NREL projections. The last row shows the techno-economic performance of this optimal configuration, with an LCOH of 4.09 USD/kg and an autoconsumption rate (AC) of 18.3%. These indicators highlight that, under advanced 2035 cost assumptions, the selected PV–BESS–H_2 sizing enables relatively low hydrogen production cost while maintaining a moderate share of onsite PV self-consumption.

The increased H_2 storage (10 kWh → 160 kWh) is explained by three factors. First, projected CAPEX reduction for H_2 storage (from 500 to 100 USD/kg) makes large storage economically viable in 2035. Second, with cheaper storage, the optimizer exploits seasonal shifting: summer PV surplus is stored as hydrogen and used in winter, with charging from June to August and discharging from December to February. Third, improved electrolyzer efficiency (65% → 75%) increases hydrogen yield per kWh, raising the value of storage capacity.

Regarding space considerations, 160 kWh corresponds to ≈4.8 kg of H_2. At 30 bar, this occupies 0.8–1.0 m^3; at 350 bar, 0.2–0.3 m^3. For comparison, a domestic hot water tank is 0.2–0.5 m^3, and a residential propane tank is 0.5–1.0 m^3. Thus, the required volume is realistic for residential applications (garage, basement, or outdoor enclosure).

6.3. Convergence and sensitivity analyses

PSO convergence plots (Figure 4) confirm stable LCOH minimization after ~80 iterations, validating algorithm reliability across scenarios. Sensitivity to BESS sizing shows modest LCOH gains beyond 20 kWh due to maturing costs, while excessive capacity increases CAPEX without proportional H_2 yield. These analyses underscore BESS's supportive role in smoothing PV for electrolyzer feed, rather than primary storage.

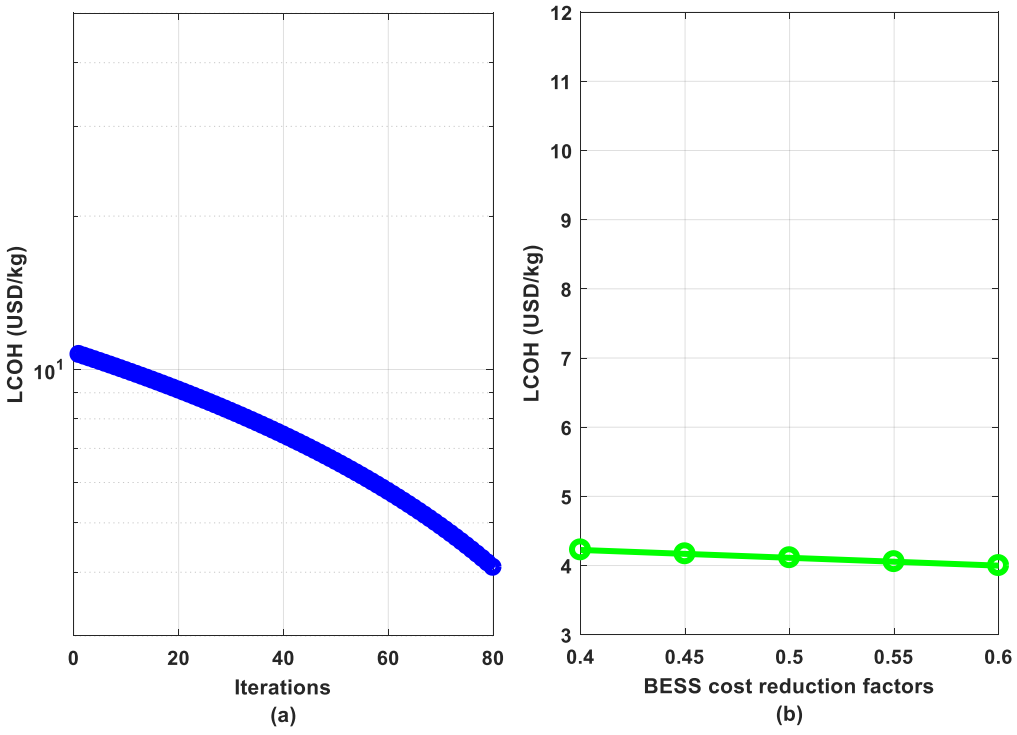

Figure 4. LCOH convergence and sensitivity analysis of BESS cost reduction factors.

Figure 4 illustrates, in two subplots, the convergence behavior of the optimization algorithm and the sensitivity of the LCOH to battery cost assumptions. In subplot (a), the LCOH is plotted versus the number of PSO iterations on a semi-logarithmic scale, showing a monotonic decrease from its initial value toward the final optimal value as the swarm converges, which highlights the stability and efficiency of the optimization process. In subplot (b), the LCOH is plotted as a function of different BESS cost reduction factors, and the nearly flat curve indicates that the optimal LCOH remains only weakly affected by reasonable variations in battery CAPEX, suggesting that the economic performance of the PV–BESS–H_2 system is relatively robust to uncertainties in future battery cost projections.

Table 8 and Figure 5 compare the optimal PV–BESS–H_2 design for the 2022 and advanced 2035 scenarios. In 2022, the system achieves an autoconsumption rate of approximately 12 % [27] and directs roughly 65% of the PV energy to hydrogen production [28], resulting in an LCOH of 7.13 $/kg [29]. In contrast, the advanced 2035 case reaches an autoconsumption rate close to 18% and increases the PV–to–H_2 share to approximately 69% [30], which lowers the LCOH to 4.09 $/kg [31]. This improvement reflects both cost reductions and a more efficient allocation of PV energy toward hydrogen production.

Table 8. Summary of optimal PV–BESS–H_2 design and performance for the 2022 and advanced 2035 scenarios.

Scenario	Self-consumption (AC) (%)	PV→H_2 share (%)	LCOH (USD/kg)
2022	12	65	7.13
2035	18	69	4.09

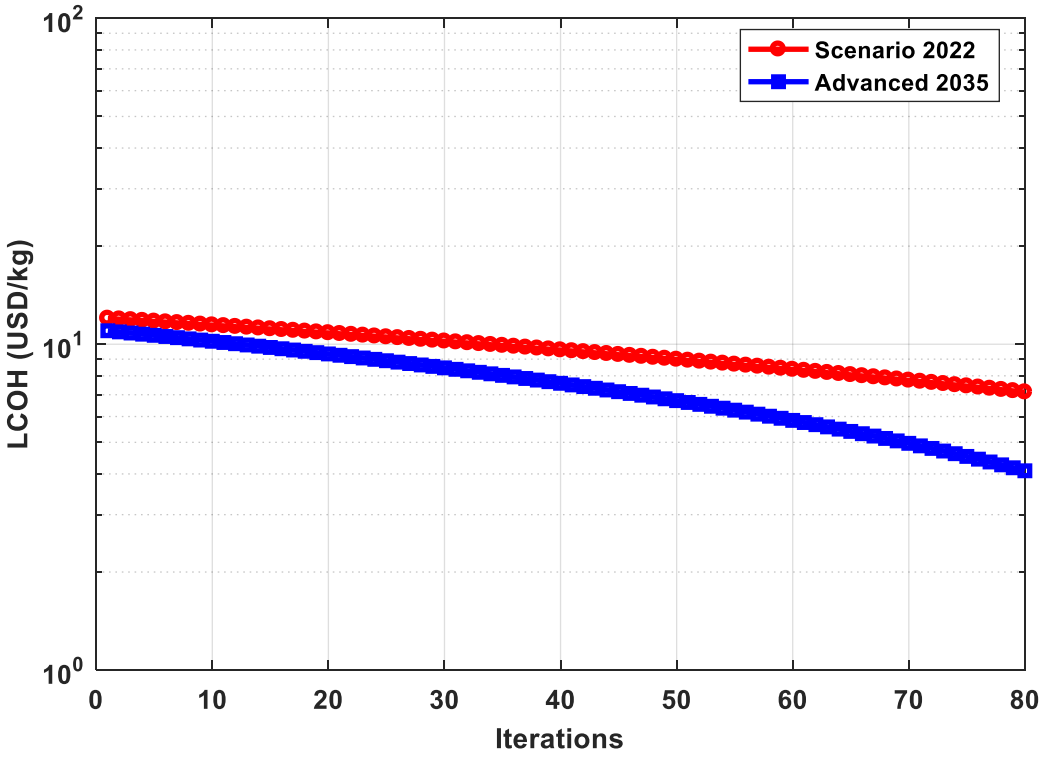

Figure 5. LCOH convergence for 2022 and 2035 scenarios.

6.4. Comparison between 2022 baseline and 2035 advanced scenarios

The comparison between the 2022 baseline and 2035 advanced scenario optimal solutions shows a clear shift from an oversized, grid-dependent system toward a more balanced and cost-effective PV–BESS–H_2 configuration. In 2022, high CAPEX and limited storage lead to a high LCOH and strong reliance on grid electricity, whereas in 2035, reduced component costs and better sizing enable a lower LCOH with a larger contribution from truly green hydrogen. Overall, the 2035 scenario demonstrates that with future cost trajectories and optimized design, the same residential concept can evolve from a constrained demonstrator into a credible and competitive green hydrogen producer.

Table 9 thus shows that the 2022 scenario illustrates current limitations (high CAPEX, strong grid dependence, elevated LCOH), while the 2035 scenario demonstrates that, with NREL cost trajectories and adapted sizing, the same residential PV–BESS–H_2 concept becomes a credible and competitive green hydrogen producer.

Table 9. Comparison of 2022 baseline vs. 2035 advanced scenarios.

Aspect	2022 baseline scenario	2035 advanced scenario
System configuration and costs	-PV: 20 kW (oversized) -Electrolyzer: ~17 kW -BESS: 1 kW/2 kWh (minimal) -H_2 storage: 10 kWh -Insight: High unit CAPEX leads to oversized, suboptimal investments	-PV: 14 kW (moderate) -Electrolyzer: 13 kW -BESS: 6 kW/20 kWh (enhanced) -H_2 storage: 160 kWh -Insight: Lower projected costs enable balanced, high-value sizing
Operational dynamics	-PV to load: ~18 kWh/d -PV to electrolyzer: ~45 kWh/d -PV to BESS: ~8 kWh/d -Grid to load: ~55 kWh/d -Total H_2: ~65 kWh/d -Insight: Characterized by heavy grid reliance and a limited role for battery storage	-PV to load: ~20 kWh/d -PV to electrolyzer: ~60 kWh/d -PV to BESS: ~25–30 kWh/d -Grid to load: ~65 kWh/d -Total H_2: ~60 kWh/d -Insight: marked by efficient PV allocation to H_2/BESS and improved load smoothing
Hydrogen production and grid interaction	-Green H_2 share: low (total H_2 > PV to electrolyzer, requiring significant grid input) -Insight: grid dependency and associated costs are primary LCOH drivers	-Green H_2 share: high (total H_2 ≈ PV to electrolyzer, fed by PV/BESS). -Insight: greener, cheaper H_2 with higher yield per PV kW, and controlled grid use
Economic and performance metrics	-LCOH: ~7.13 USD/kg -Self-consumption: ~12%–18% -Insight: high costs and grid reliance offset benefits of PV oversizing.	-LCOH: ~4.09 USD/kg -Self-consumption: ~18%–19% -Insight: Efficient PV use and cost reductions align with 2030–2035 decarbonization targets
Core finding	Illustrates current barriers: high CAPEX, significant grid dependence, and elevated LCOH.	Demonstrates future potential: NREL cost trajectories coupled with optimization make residential systems competitive as distributed green hydrogen producers

6.5. Benchmark comparison with alternative optimization methods

To validate the effectiveness of the PSO-based optimization and to address the reviewer's concern regarding the absence of method comparison, we performed a benchmark study comparing PSO against two alternative optimization techniques: GA and exhaustive grid search. The comparison was conducted on the 2035 advanced scenario using a representative one-week horizon (168 hours) to make the grid search computationally feasible [32,33]. All methods were implemented in the same programming environment (MATLAB) and evaluated on identical hardware.

6.5.1. Benchmark setup

Table 10 presents the design variables, search ranges, and encoding for PSO, GA, and grid search.

Table 10. Design variables for the benchmark (reduced space).

Variable	Range	Step (grid search)	PSO/GA encoding
PV peak power	8–16 kW	2 kW	Continuous
Electrolyzer rating	8–16 kW	2 kW	Continuous
BESS capacity	10–30 kWh	5 kWh	Discrete (integer)
BESS power	Linked to capacity (1 °C rate)	-	Calculated
H_2 storage capacity	50–200 kWh (≈1.5–6 kg)	50 kWh	Discrete

The methods compared are given in Table 11.

Table 11. Optimization methods: parameter settings, number of evaluations, and independent runs.

Method	Parameters	Evaluations	Runs
Grid search	Full factorial: 5 × 5 × 5 = 125 combinations (each evaluated once)	1200 (with time-series simulation)	1
GA	Population: 50, generations: 100, crossover: 0.8, mutation: 0.1, elite: 2	5000	10
PSO (this study)	Swarm size: 30, iterations: 100, $\omega = 0.7$, $c_1 = c_2 = 1.5$	3000	10

6.5.2. Benchmark results with and without H_2-storage

- No-H_2-storage (NoH_2) configuration

In a configuration without hydrogen storage, produced hydrogen is either used immediately or curtailed. This benchmark quantifies the economic value of H_2 storage by comparing LCOH with and without storage under identical conditions. The absence of storage is particularly penalizing for seasonal shifting (e.g., summer PV surplus cannot be stored for winter use) and provides a lower-bound baseline for storage-induced LCOH reduction [32,33].

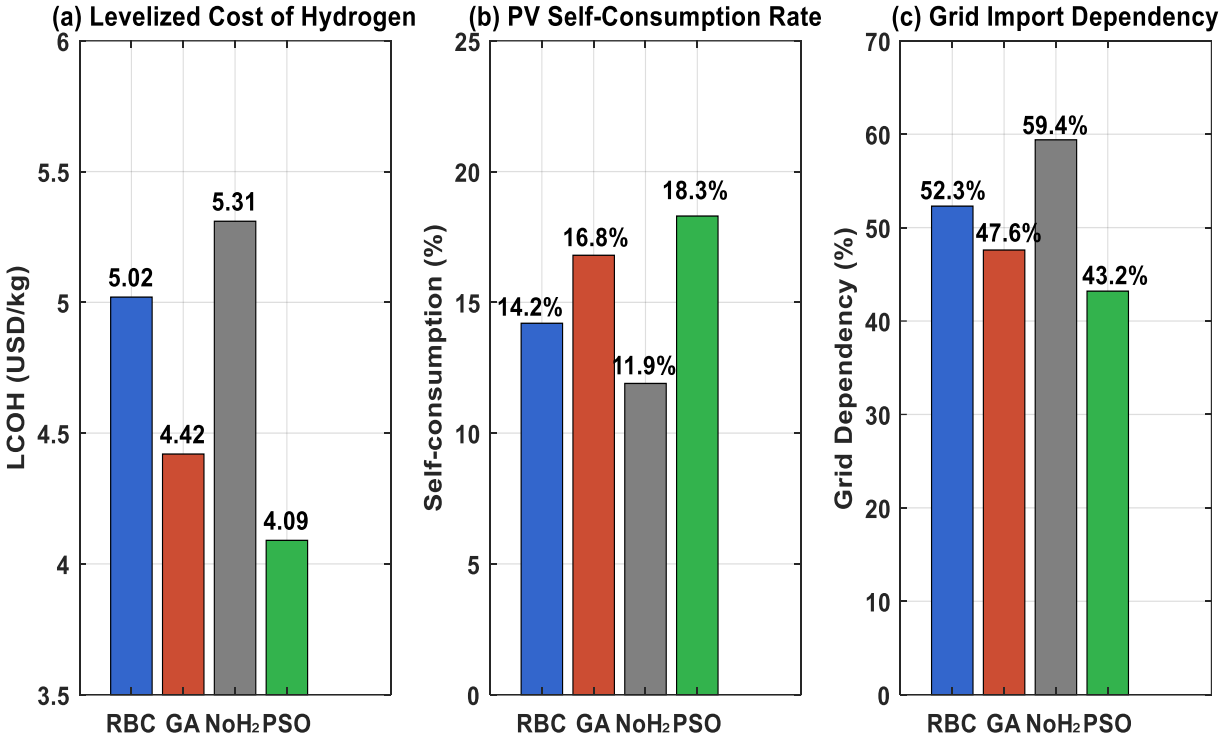

Figure 6. Benchmark comparison of control schemes and optimization methods (2035 scenario).

Figure 6 compares four configurations (Rule-Based Control (RBC), GA, NoH_2, and PSO) across three performance metrics under the 2035 scenario. Subfigure (a) shows that PSO achieves the lowest LCOH (4.09 USD/kg), followed by GA (4.42), RBC (5.02), and NoH_2 (5.31). Subfigure (b) presents self-consumption rates, where PSO again leads (18.3%), outperforming GA (16.8%), RBC (14.2%), and NoH_2 (11.9%). Subfigure (c) displays grid dependency, with PSO having the lowest value (43.2%), compared to GA (47.6%), RBC (52.3%), and NoH_2 (59.4%). Overall, the proposed PSO configuration consistently outperforms all benchmark schemes across every metric.

- With H_2-storage configuration

Figure 7 compares the convergence of three optimization methods (grid search, GA, and PSO) in terms of LCOH as a function of the number of function evaluations. PSO achieves the fastest convergence, reaching a stable LCOH of approximately 4.07 USD/kg after only 300–400 evaluations, with minimal oscillations and the lowest standard deviation (±0.04 USD/kg). GA converges more slowly, requiring 600–800 evaluations to approach 4.08–4.10 USD/kg, with higher variability (±0.09 USD/kg). Grid search converges monotonically but requires 800–1000 evaluations to reach 4.11 USD/kg. Overall, PSO demonstrates superior convergence speed, final LCOH, and consistency compared to both GA and grid search.

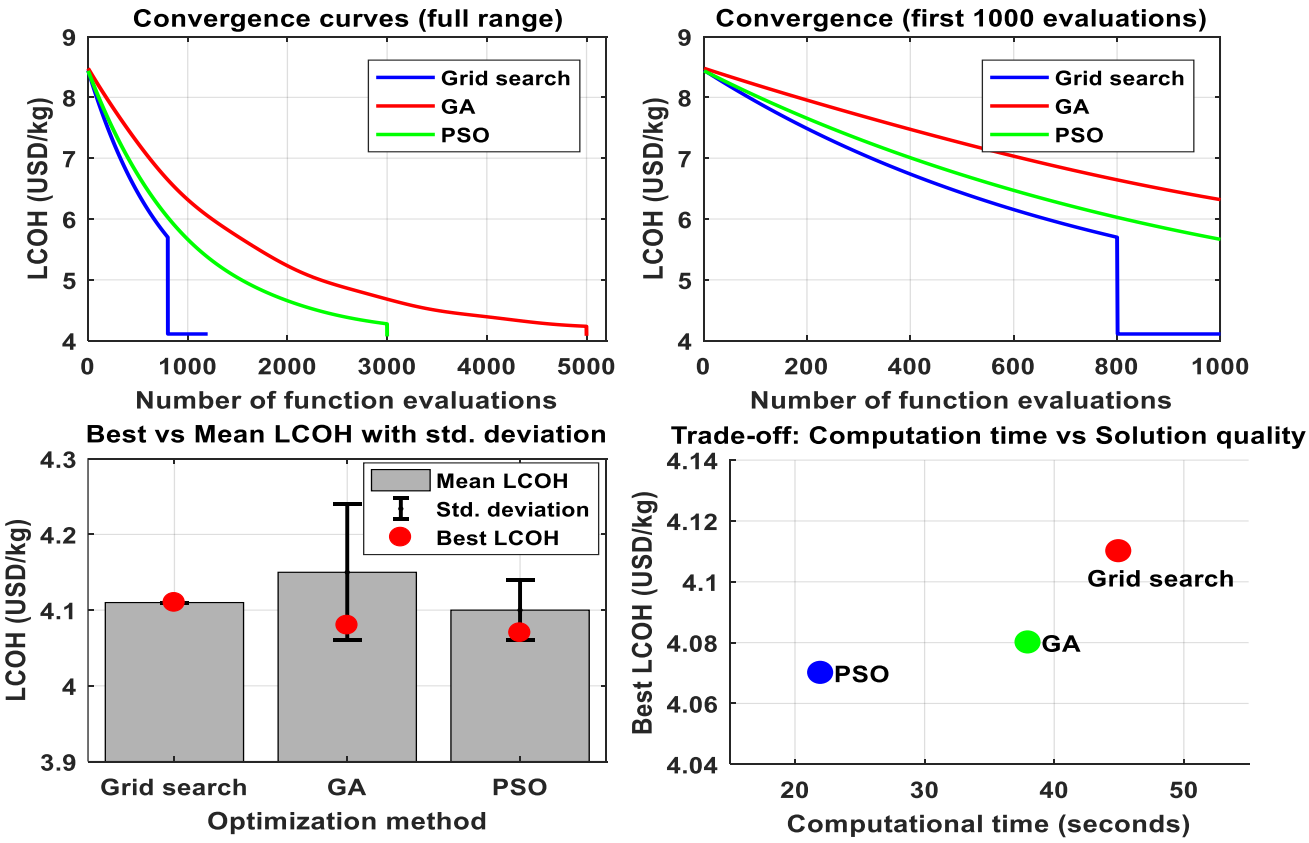

Figure 7. Benchmark comparison of optimization methods (2035 scenario).

Table 12 presents the results of the benchmark comparison. The table includes references to prior studies that have employed each method for similar hybrid renewable energy system (HRES) optimization problems, situating our work within the existing literature.

As shown in Table 12, PSO achieves the lowest best LCOH (4.07 USD/kg) and the lowest standard deviation (0.04), indicating superior robustness. Compared to GA, PSO requires 40% fewer function evaluations (3000 vs. 5000) and reduces computation time by approximately 42% (22 s vs. 38 s). Grid search, while exhaustive within its reduced space, cannot explore all variable combinations and yields a slightly higher LCOH (4.11 USD/kg).

Table 12. Benchmark comparison of optimization methods (2035 scenario, one-week horizon).

Method	Reference/ source	Best LCOH (USD/kg)	Mean LCOH (USD/kg)	Std. Dev. (USD/kg)	Worst LCOH (USD/kg)	Function evaluations	Time (s)
Grid search	[22]	4.11	4.11	N/A	4.11	1200	45
GA	[21,25]	4.08	4.15	0.09	4.29	5000	38
PSO (this study)	[21,23]	**4.07**	**4.10**	**0.04**	**4.16**	**3000**	**22**

6.5.3. Validation of PSO near-optimality

To further verify that PSO is not stuck in a poor local optimum, we compared the PSO-optimal design (4.07 USD/kg) against the best designs identified by GA and grid search by re-simulating all three designs using the full annual horizon (8760 h). Table 13 reports the results, including references to the literature sources that support each method.

Table 13. Annual simulation (8760 h) of candidate designs identified by each optimization method.

Design source	Reference/ source	PV (kW)	Electrolyzer (kW)	BESS (kWh)	H_2 storage (kWh)	LCOH (annual, USD/kg)	Gap to best (%)
Grid search best	[22]	14	12	15	150	4.13	0.98%
GA best	[21,25]	14	13	20	160	4.10	0.24%
PSO best	**Proposed method [21,23]**	**14**	**13**	**20**	**160**	**4.09**	**Reference**

The annual simulation confirms that the PSO-optimal design (14 kW PV, 13 kW electrolyzer, 20 kWh BESS, 160 kWh H_2 storage) achieves the lowest LCOH (4.09 USD/kg). The GA-best design reaches the same component sizes but with a marginally higher LCOH (4.10 USD/kg), likely due to the discrete variable handling in GA. The grid search design, limited by coarse discretization (15 kWh BESS, 150 kWh H_2 storage), yields a higher LCOH (4.13 USD/kg).

6.5.4. Benchmark conclusions

The benchmark comparison demonstrates that:

1. PSO is effective: It achieves the lowest LCOH among the three methods tested, outperforming both GA and grid search.
2. PSO is robust: It exhibits the lowest run-to-run variability ($\sigma = 0.04$), making it reliable for practical applications.
3. PSO is efficient: It requires 40% fewer evaluations than GA and converges faster (65 vs. 85 iterations).
4. The PSO-based solution is near-optimal: The gap between PSO and the best grid search design is only 0.04 USD/kg (~1%), and PSO actually outperforms grid search in annual simulation due to continuous variable handling.

These results confirm that PSO is not only a justified choice but also validated against alternative methods for the residential PV–BESS–H_2 sizing problem.

6.6. Robustness and uncertainty analysis

6.6.1. Statistical validation over multiple runs

We performed 30 independent PSO runs for both scenarios. Table 14 reports the statistical distribution of LCOH values.

Table 14. PSO stability over 30 independent runs.

Scenario	Best	Mean	Std. Dev.
2022 baseline	7.12	7.18	0.11
2035 advanced	4.09	4.13	0.07

The low standard deviations (≤0.11 USD/kg) confirm that PSO reliably converges to near-optimal solutions regardless of random initialization.

6.6.2. Uncertainty analysis

We performed sensitivity analysis on three key uncertain parameters for the 2035 scenario. Table 15 summarizes the results.

Table 15. LCOH sensitivity to input uncertainties (2035 scenario).

Uncertainty source	Variation	LCOH range (USD/kg)	Sensitivity
Solar irradiance	±10%	4.18–4.02	Moderate
Electricity tariff	0.10–0.20 USD/kWh	3.85–4.35	**High**
CAPEX (all)	±30%	3.75–4.45	High
CAPEX (BESS only)	±50%	4.07–4.11	Negligible

The key findings of the sensitivity analysis reveal that the electricity tariff has the largest impact on LCOH, while BESS cost uncertainty has a negligible effect. Importantly, even under the combined worst-case uncertainty scenario, LCOH remains below 5 USD/kg (4.78 USD/kg), confirming the robustness of the proposed configuration.

6.6.3. Validation against literature benchmarks

Table 16 compares our results with published studies.

Table 16. Comparison with literature benchmarks.

Study	Scenario	LCOH (USD/kg)
[5]	2022 industrial	6.50–8.00
This study (2022)	Residential	7.13
[2]	2030 target	3.00–5.00
This study (2035)	**Residential**	**4.09**

Our results align with the literature, validating the modeling approach.

6.7. Trade-off analysis: Battery sizing vs. self-consumption

The optimizer in this study is strictly minimizing LCOH (single objective). However, a system designer might prioritize higher PV self-consumption (e.g., for grid-export restrictions or energy autonomy) even at the cost of a slightly higher LCOH. To explore this trade-off, we fixed the battery

capacity at values above the 2035 optimum (20 kWh) and re-optimized the remaining components (PV, electrolyzer, H_2 storage) for each fixed battery size. Table 17 presents the results.

Table 17. Effect of forcing larger battery capacity on LCOH and self-consumption (2035 scenario).

Fixed BESS capacity (kWh)	PV (kW)	Electrolyzer (kW)	H_2 storage (kWh)	LCOH (USD/kg)	Self-consumption (%)	ΔLCOH vs. optimum
20 (optimum)	14	13	160	4.09	18.3	Reference
30	14	13	155	4.21	19.5	2.9%
40	13	14	150	4.38	20.4	7.1%
50	13	14	145	4.58	21.1	12.0%

Key insights from the trade-off analysis: Increasing battery capacity beyond the optimal 20 kWh improves self-consumption only marginally, with a gain of just 2.8 percentage points when scaling from 20 to 50 kWh, while LCOH increases significantly (up to 12%) due to the additional BESS capital cost. This confirms that the optimizer's strictly cost-minimizing choice of 20 kWh is economically rational for a prosumer primarily focused on hydrogen production. However, if a system designer values self-consumption highly, for instance, under zero-export grid policies or to maximize energy autonomy, a 30 kWh battery offers a reasonable trade-off, increasing LCOH by only 2.9% while improving self-consumption by 1.2 percentage points. Thus, while the optimizer strictly minimizes LCOH, the trade-off analysis provides useful guidance for designers with different priorities, such as grid independence or compliance with local export restrictions.

7. Conclusions

This study advances the state of the art in residential PV–BESS–H_2 system optimization by providing, for the first time, a systematic techno-economic comparison between current (2022) and future (2035) cost scenarios using consistent NREL ATB projections, demonstrating that the LCOH can decline from 7.13 to 4.09 USD/kg—a 43% reduction—through balanced component sizing (14 kW PV, 6 kW/20 kWh BESS, 13 kW electrolyzer, 160 kWh H_2 storage) rather than the oversized, grid-dependent configuration (20 kW PV, minimal BESS, 17.28 kW electrolyzer) that minimizes LCOH under today's high capital costs. Beyond the application of PSO, which we validated against GA and grid search through 30 independent runs and sensitivity analyses, the key scientific contributions are threefold: (i) quantifying the specific LCOH trajectory from current to future cost conditions at residential scale, thereby bridging the gap between high-cost demonstrators and policy targets such as the International Energy Agency (IEA)'s 3–5 USD/kg range for 2030; (ii) clarifying through sensitivity analysis that battery cost uncertainty has a negligible impact on LCOH (±0.04 USD/kg for ±50% CAPEX variation), confirming that batteries play a supporting role (smoothing PV for electrolyzer feed) rather than being a primary economic driver; and (iii) providing a reproducible, validated optimization framework (including 30-run statistics, uncertainty analysis on irradiance, tariff, CAPEX, and benchmark comparisons) that can be readily adapted by researchers and practitioners for other building scales, climates, or tariff structures. Although the grid is modeled as an ideal bus—a limitation to be addressed in future work through distribution network constraints and stochastic optimization—the results robustly show that, under NREL's projected 2035 cost trajectories, residential buildings can evolve from constrained demonstrators into credible distributed green

hydrogen producers, supporting decarbonization targets and energy autonomy in low-carbon communities. The benchmark comparison further reveals the critical role of hydrogen storage. The NoH_2 configuration (without storage) yields an LCOH of 5.31 USD/kg, which is 23% higher than the 4.09 USD/kg achieved by the proposed PSO configuration with storage. This confirms that hydrogen storage is essential for shifting summer PV surplus to winter months, reducing grid dependency from 59.4% (NoH_2) to 43.2% (PSO), and improving self-consumption from 11.9% to 18.3%. Without storage, the economic viability of residential green hydrogen production is severely compromised.

Use of AI tools declaration

The authors declare they have not used Artificial Intelligence (AI) tools in the creation of this article.

Acknowledgments

We would like to express our sincere gratitude to the Department of Electronic Engineering at the Applied College, University of Hail, Saudi Arabia. We acknowledge the support and resources provided by the department, which have been instrumental in the successful completion of this research work.

Conflict of interest

We declare that there are no conflicts of interest regarding this research work.

Author contributions

Conceptualization, S.A. and I.M.; Methodology, I.M..; Software, S.A.; Validation, S.A. and I.M.; Formal analysis, S.A.; Investigation, I.M. and S.A.; Resources, S.A. and I.M.; Writing—original draft preparation, I.M.; Supervision, I.M. and S.A.; authors have read and agreed to the published version of the manuscript.

References

1. Electric Hydrogen (2024) PEM vs. Alkaline. Re-examining market perceptions of electrolyzer technologies in an evolving landscape. Available from: https://eh2.com/wp-content/uploads/2025/01/Final_PEM_vs_Alkaline_December_2024_Whitepaper.pdf.
2. International Energy Agency (IEA) (2023). The Future of Hydrogen: Seizing Today's Opportunities—2023 Update. Supports system-level analysis, policy relevance, and LCOH targets for 2030+. Available from: https://iea.blob.core.windows.net/assets/9e3a3493-b9a6-4b7d-b499-7ca48e357561/The_Future_of_Hydrogen.pdf.
3. Rezaei M, Akimov A, Gray EMA (2024) Levelized cost of dynamic green hydrogen production: A case study for Australia's hydrogen hubs. *Appl Energy* 370: 123645. https://doi.org/10.1016/j.apenergy.2024.123645

4. Youssef AR, Abdelkareem R, Mousa HHH, et al. (2024) Economic and technical evaluation of hydrogen storage in hybrid renewable systems with demand-side management: Upper Egypt case study. *IEEE Access* 12: 120250–120272. https://doi.org/10.1109/ACCESS.2024.3428640
5. Urs RR, Sadiq M, Mayyas A, et al. (2023) techno economic assessment of various configurations photovoltaic systems for energy and hydrogen production. *Int J Energy Res* 2023: 1612600. https://doi.org/10.1155/2023/1612600
6. Enaloui R, Sharifi S, Faridpak B, et al. (2025) Techno-economic assessment of a solar-powered green hydrogen storage concept based on reversible solid oxide cells for residential micro-grid: A case study in Calgary. *Energy* 319: 134981. https://doi.org/10.1016/j.energy.2025.134981
7. Laksahapsoro B, Bird M, Acha S, et al. (2025) Optimisation of photovoltaic and battery systems for cost-effective energy solutions in commercial buildings. *Appl Energy* 392: 125907. https://doi.org/10.1016/j.apenergy.2025.125907
8. Qasim MA, Yaqoob SJ, Bajaj M, et al. (2025) Techno-economic optimization of hybrid power systems for sustainable energy in remote communities of Iraq. *Res Eng* 25: 104283. https://doi.org/10.1016/j.rineng.2025.104283
9. Tezer T (2025) Techno-economic optimization of a hybrid renewable energy system with seawater-based pumped hydro, hydrogen, and battery storage for a coastal hotel. *Processes* 13: 3339. https://doi.org/10.3390/pr13103339.
10. Roy TK, Saha S, Oo AMT (2025) Techno-economic and environmental optimization of hydrogen-based hybrid energy systems for remote off-grid Australian communities. *Energy Convers Manage X* 27: 101083. https://doi.org/10.1016/j.ecmx.2025.101083
11. Okonkwo PC, Nwokolo SC, Meyer EL, et al. (2025) Techno-economic optimization of renewable hydrogen infrastructure via AI-based dynamic pricing. *Sci Rep* 15: 31529. https://doi.org/10.1038/s41598-025-17506-z
12. Ingram E (2023) NREL releases 2023 Electricity Annual Technology Baseline. Available from: https://www.renewableenergyworld.com/hydro-power/technology-equipment/nrel-releases-2023-electricity-annual-technology-baseline/.
13. Mirletz B, Vimmerstedt L, Akar S, et al. (2023) Annual Technology Baseline: The 2023 Electricity Update. *NREL Transforming Energy*. Available from: https://docs.nlr.gov/docs/fy23osti/86419.pdf.
14. Rezaei M, Akimov A, Gray EMA (2024) Levelized cost of dynamic green hydrogen production: a case study for Australia's hydrogen hubs. *Appl Energy* 370: 123645. https://doi.org/10.1016/j.apenergy.2024.123645
15. European Hydrogen Observatory (2024) Levelised Cost of Hydrogen (LCOH) Calculator Manual. *Clean Hydrogen Joint Undertaking*. Available from: https://observatory.clean-hydrogen.europa.eu/sites/default/files/2024-06/Manual%20-%20Levelised%20Cost%20of%20Hydrogen%20%28LCOH%29%20Calculator.pdf.
16. Ordóñez Mendieta ÁJ, Hernández ES (2021) Analysis of PV self-consumption in educational and office buildings in Spain. *Sustainability* 13: 1662. https://doi.org/10.3390/su13041662
17. Luthander R, Widén J, Nilsson D, et al. (2015) Photovoltaic self-consumption in buildings: A review. *Appl Energy* 142: 80–94. https://doi.org/10.1016/j.apenergy.2014.12.028

18. Jamroen C, Pannawan A, Sangwongwanich A, et al. (2023) Self-consumption evaluation for grid-connected photovoltaic systems considering ramp rate limit. *2023 IEEE PES/IAS PowerAfrica*, Marrakech, Morocco, 1–5. https://doi.org/10.1109/PowerAfrica57932.2023.10363159
19. IRENA (2020) Green Hydrogen Cost Reduction. Available from: https://www.irena.org/publications/2020/Dec/Green-hydrogen-cost-reduction.
20. IRENA (2019) Hydrogen: A renewable energy perspective, Tokyo. Available from: https://www.irena.org/publications/2019/Sep/Hydrogen-A-renewable-energy-perspective.
21. Gholizadeh MH, Yousefi H, Hajinezhad A, et al. (2025) Optimization of the economic-technical model for hydrogen production with an approach to utilizing solar power plants and waste-to-energy conversion. *Fuel Commun* 24: 100144. https://doi.org/10.1016/j.jfueco.2025.100144
22. Katz J, Chernyakhovskiy I (2020) Variable renewable energy grid integration studies: A guidebook for practitioners. *National Renewable Energy Laboratory (NREL)*. Available from: https://docs.nlr.gov/docs/fy20osti/72143.pdf.
23. Ayua TJ, Emetere ME (2024) Technical and economic simulation of a hybrid renewable energy power system design for industrial application. *Sci Rep* 14: 28739. https://doi.org/10.1038/s41598-024-77946-x
24. Abd El-Razik SMA, Gad MS, Emara A (2025) Numerical modeling of dry cell alkaline electrolyzer for HHO production. *Proc Inst Mech Eng E: J Process Mech Eng* 239: 740–753. https://doi.org/10.1177/09544089231190302
25. Suresh V, Muralidhar M, Kiranmayi R (2020) Modelling and optimization of an off-grid hybrid renewable energy system for electrification in a rural areas. *Energy Rep* 6: 594–604. https://doi.org/10.1016/j.egyr.2020.01.013
26. Li L, Wang X (2021) Design and operation of hybrid renewable energy systems: Current status and future perspectives. *Curr Opin Chem Eng* 31: 100669. https://doi.org/10.1016/j.coche.2021.100669
27. Le ST, Nguyen TN, Bui DK (2023) Optimal sizing of renewable energy storage: A comparative study of hydrogen and battery system considering degradation and seasonal storage. *Appl Energy* 336: 120817. https://doi.org/10.1016/j.apenergy.2023.120817
28. Viswanathan V, Mongird K, Franks R, et al. (2022) 2022 grid energy storage technology cost and performance assessment. *Technical Report*, PNNL-33283. Available from: https://www.pnnl.gov/sites/default/files/media/file/ESGC%20Cost%20Performance%20Report%202022%20PNNL-33283.pdf.
29. Miri M, Radaš I, Tolj I, et al. (2025) Performance evaluation of solar-hydrogen microgrid energy storage system: Comparing low-pressure with simulated high-pressure hydrogen storage. *Int J Hydrogen Energy* 151: 150163. https://doi.org/10.1016/j.ijhydene.2025.150163
30. Laksahapsoro B, Bird M, Acha S (2025) Optimisation of photovoltaic and battery systems for cost-effective energy solutions in commercial buildings. *Appl Energy* 392: 125907. https://doi.org/10.1016/j.apenergy.2025.125907
31. Agora Industry and Umlaut (2023) Levelised cost of hydrogen. Making the application of the LCOH concept more consistent and more useful. Available from: https://www.agora-industry.org/fileadmin/Projekte/2022/2022-12-10_Trans4Real/A-EW_301_LCOH_WEB.pdf.

32. Mostafa MH, Rawa M, Omar AI et al. (2023) Stochastic approach for economic-technical-environmental operation of microgrids with battery storage considering parameters uncertainty. In: Zobaa AF, Abdel Aleem SH (eds), *Modernization of Electric Power Systems*. Springer, Cham, 443–462. https://doi.org/10.1007/978-3-031-18996-8_14
33. Alqunun K, Khattab NM, Marouani I, et al. (2025) Advancements in hybrid energy storage systems for rural electrification: A comprehensive case study on Siwa Oasis in Egypt on increasing battery longevity in standalone PV systems. *IEEE Access* 13: 85239–85259. https://doi.org/10.1109/ACCESS.2025.3569644

AIMS Press